ASIAN JOURNAL OF PHARMACEUTICAL AND CLINICAL RESEARCH

INNOVARE ACADEMIC SCIENCES
Knowledge to Innovation

Vol 10, Issue 3, 2017

Online - 2455-3891
Print - 0974-2441

Research Article

EVALUATION OF ANTIMICROBIAL ACTIVITY OF GREEN-SYNTHESIZED MANGANESE OXIDE NANOPARTICLES AND COMPARATIVE STUDIES WITH CURCUMINANILINE FUNCTIONALIZED NANOFORM

MUHAMED HANEEFA M[1]*, JAYANDRAN M[2], BALASUBRAMANIAN V[1]

[1]Department of Chemistry, AMET University, Chennai, Tamil Nadu, India. [2]Department of Chemistry, Thiruvalluvar Government Arts College, Namakkal, Tamil Nadu, India. Email: honey79101@gmail.com

Received: 20 November 2016, Revised and Accepted: 06 December 2016

ABSTRACT

Objective: Metal oxide nanoparticles are widely attracted researchers due to their potential applications in a variety of fields, especially medicinal importance. It has been shown that biofunctionalization of metal nanoparticles with the specified bioactive materials produces the significantly improved bioactive materials with the essential biological properties and advanced features. According to the reports, manganese oxide nanoparticles (MONPs) possess highly magnetic properties leads to develop for use in research and biomedical applications. In this evaluation, we focused on the synthesis of MONPs through a green methodology and their antimicrobial activity changes when functionalized with curcuminaniline derived from turmeric plants.

Methods: First, curcumin has been isolated from turmeric plant (BSR-01) to synthesize curcuminaniline biomaterial. On the other hand, manganese nanoparticles are synthesized by the green synthesis method using lemon extract and curcumin. Finally, the synthesized curcuminaniline is functionalized with MONPs. The synthesized nanoparticles are characterized by ultraviolet-visible, Fourier transform infrared, scanning electron microscope and transmission electron microscopy techniques. The antimicrobial activity of the obtained nonfunctionalized and biofunctionalized nanoforms are tested against some Gram-negative and Gram-positive bacterial strains as well as fungal strains.

Results: The morphological studies represented that MONPs are of eclipsed and spherical morphology with size about 50±5 nm and biofunctionalized nanoparticles are of spherical morphology with size about 50±10 nm. The antibacterial and antifungal tests revealed that biofunctionalized MONPs are exhibited significantly higher antimicrobial activity.

Conclusion: This investigation clearly demonstrated that MONPs are shown significantly higher biocidal activity when biofunctionalized with modified curcumin material. This may help in the future medicinal and pharmaceutical industries to develop new inventions.

Keywords: Green synthesis, Nanoparticles, Curcumin, Curcuminaniline, Soxhlet extraction, Antimicrobial activity.

 DOI: http://dx.doi.org/10.22159/ajpcr.2017.v10i3.16246

INTRODUCTION

During the last years, nanotechnology has been widely favored due to its growing interest on the matter at nanoscale and its advanced properties. The field of nanomaterials has been the key feature among the scientists due to its unique physical, chemical, and effective biological properties [1,2]. It is known that the phases, sizes, morphology, and dimensionality of the nanomaterial have great influence on the modifications of properties and functionalities. Hence, many research efforts have focused to control such important factors to attain the featured nanomaterials [3]. Moreover, synthesis of nanoparticles in the eco-friendly green synthesis method is challenging aspect in current nanotechnology. Nanoparticles are often prepared by conventional methods which are producing hazardous derivatives and harmful to the environment. Therefore, scientists are giving high priority to green synthesis methods in the nanoparticle preparation at present [4,5].

The severe increasing resistance to existing antibiotics of various microbes, researchers have turned toward engineered nanoparticles for finding a proactive antibiotic. Nanotechnology is currently employed as a tool to discover the advancement in the biomedical sciences because metal and metal oxide nanoparticles have been shown considerable bactericidal effects and can use for the treatment of various applications such as diagnosis of diseases, drug delivery systems, and sun screens [6-8]. Organic disinfectants have some toxicity to the human body, which increased the interest in inorganic disinfectants such as metal oxide nanoparticles at present. The antimicrobial activity of metal oxide nanoparticles is due to the large surface area which ensures a comprehensive range of reactions with bio-organics materials existing on the cell surface [9-11].

During the past few years, magnetic behavioral nanomaterials have attracted the researchers due to their promising applications in wide areas such as magnetic data storage, gas sensors, targeted drug delivery, and magnetic resonance imaging [12-15]. As an important functional magnetic natured metal oxide, manganese oxide has attracted extensive research interest due to their significant distinctive physical, chemical properties, electrical, magnetic and catalytic properties different from that of bulky materials [16,17]. According to literature, manganese oxide nanoparticles (MONPs) has offered significant potentials in many fields such as catalysis, ion exchange, molecular adsorption, energy storage, chemical, and biological sensing [18-22]. In the case of MONPs, most of the reports were focused on the characterization and application of the formed manganese nanoparticles in catalytic activity, electronic properties, but the antimicrobial activity of manganese nanoparticles was investigated very rarely. In this investigation, nanosized manganese nanoparticles are considered to establish its antimicrobial activity as well as its improvement in the activity after a biofunctionalization process with selected biomaterial.

Biofunctionalization of nanomaterials is one such topic focused by recent researches due to the ability to produce the nontoxic and

highly efficient antimicrobial agents in terms of green nanotechnology. Biofunctionalization of nanoparticles is an advancement of current nanotechnology and biotechnology fields. In which, the possibilities of nanoparticle modification by interacting with biologically active compounds to use them in various biological activities are very interesting. However, the selection of active biomolecules to design the functionalized nanoparticles will be a crucial matter in this field [23-25]. Plants are used medicinally in different biological processes and are a source of many potent and powerful drugs. Curcumin (*Curcuma longa*) is well established biologically active natural material derived from turmeric plants. Curcumin has been shown to exhibit various potential applications in medicinal chemistry [26-28]. Some researchers were proved that functionalization of modified curcumin has been exhibited better biological activities than raw curcumin. Patra *et al*. (2016) synthesized curcumin functionalized AgNPs which has been shown to have significant antibacterial activities. Moussawi and Patra (2015) prepared zinc oxide nanoparticles by the surface modification of curcumin which possessed an effective arsenic removal property in water purification. Furthermore, we synthesized curcumin functionalized copper, zinc and iron oxide nanoparticles with highly enhanced antimicrobial property by the surface functionalization of modified curcumin [29-31].

In continuation with our previous works, this study based on the investigation of the antimicrobial behavior of MONPs prepared by green synthesis method. In this method, lemon extract (*Citrus limon*) has been used as a reducing agent which are rich sources of citric acid and ascorbic acid and the extracts of lemon is low pH which makes it the antibacterial active source and other useful medicinal purposes [32,33]. Turmeric curcumin has been used as a capping agent for MONPs. The synthesized MONPs were biofunctionalized with modified curcumin biomaterial, curcuminaniline. The antimicrobial activity of the nonfunctionalized as well as biofunctionalized MONPs were investigated against Gram-positive bacteria (*Staphylococcus aureus, Bacillus subtilis*), Gram-negative bacteria (*Escherichia coli, Salmonella typhi*) and some funguses (*Candida albicans*, *Curvularia lunata*, *Aspergillus niger,* and *Trichophyton simii*). The results were represented that biofunctionalized manganese oxide nanoparticles (MNCA) have displayed extremely higher antibacterial and antifungal activity against bacterial and fungal strains tested here.

METHODS

All the chemicals and solvents used were of analytical reagent grade and obtained from Merck (India) Ltd. The turmeric sample (BSR-01) was purchased from Agricultural College and Research Institute, Madurai, India.

Extraction of plant materials

Extraction of plant materials is the important step in the plant mediated green synthesis method. The selection of a suitable extraction method depends mainly on the work to be carried out and obtaining the pure form of extracts is also a crucial thing in the extraction method.

Lemon fruits were collected from the local markets and washed well with water, cut into pieces and squeezed well to make 5-10 ml pure extract. The extract was heated slightly and then filtered using Whatman's No. 1 filter paper. The filtrate was collected in a clean dried container and it was stored for further uses.

Curcumin has been extracted from turmeric in a several effective methods. However, soxhlet extraction method is one of the best routes to extract the curcumin. The main advantage of soxhlet extraction is that it is a simple and continuous process in which the extraction and filtration of the product is involved in a single step. Moreover, this method is preferred for less solubility material like curcumin and consuming a small amount of solvent to dissolve the bulk amount of material for recycling. According to the method of Manjunath *et al*. 1991 [34], the required amount of dried turmeric (BSR-01) was placed in a cellulose thimble in the soxhlet extraction chamber, which was placed on top of a collecting flask beneath a reflux condenser. The solvent material, 95% ethanol was added to the flask in the ratio of 1:50 and the set up was heated under reflux about 3 hrs. The extraction process was carried out till the color changes have been observed to pale yellow-colored mixture which showed the completion of isolation process. The extract was filtered and evaporated to dryness. The dried curcumin was collected and recrystallized to pure form.

Synthesis of curcuminaniline

Curcuminaniline synthesis process was carried out by the normal reflux method in which the synthesized curcumin was condensed with aniline and yielded the desired product. The dried pure form of curcumin (10 mmol) powder was dissolved using 95% ethanol with constant stirring till the complete dissolved solution. The prepared yellowish curcumin extract was mixed with the freshly prepared 10 mmol of aniline and stirring was continued. The mixture color got changed to an orange and it was kept for reflux at 50°C for 3-4 hrs. Finally, the orange-colored fine crystal precipitate of curcuminaniline was obtained and it was cooled, filtered. The obtained product was washed well often to remove any unreacted chemicals and dried in a vacuum oven to dryness [35].

Synthesis of MONPs

In this part, MONPs were prepared from manganese acetate via reducing it by lemon extract and stabilizing by curcumin extract. Even though lemon extract can act as both reducing and capping agent, curcumin was brought together with lemon extract to increase the stabilization of nanoparticles. 1 mmol of manganese salt solution was freshly prepared using manganese acetate.10 ml of lemon extract was added to the manganese aqueous solution with constant stirring. The pH of the solution was adjusted to mild acidic condition to get the proper result. The mixture was kept on hot magnetic stirrer at 50-60°C for an hour and the color of the mixture was changed from pale green to pale yellow which indicated the reduction of manganese metal. Curcumin extract (1 mmol) was freshly prepared by dissolving it in 95% ethanol and the yellow-colored solution was mixed with above-reduced manganese metal ion mixture. The solution was maintained at the same temperature and stirring was continued for about 2 hrs. The mixture color was changed slowly to yellowish brown and then to permanent reddish brown color which denoted the completion of the stabilization process. The final solution was centrifuged and washed several times to obtain the pure MONP and kept in the oven to dryness.

Biofunctionalization of manganese oxide nanoparticles (MNCA)

Biofunctionalization process is the final and important step in the synthesis method. It was carried out to increase the antimicrobial activity of the synthesized MONPs. The surface functionalization was carried out by the normal interaction of synthesized curcuminaniline with MONPs. 1 mmol of the synthesized curcuminaniline solution was prepared using 95% ethanol with constant stirring to get completely dissolved solution. Then, it was mixed slowly with the 1 mmol of above synthesized MONPs. The reaction mixture was kept on hot magnetic stirrer at 60°C for an hour. The brown color was slowly changed to permanent reddish brown which denoted the functionalization of curcuminaniline with MONPs. The mixture was centrifuged and washed several times and kept to dryness for further spectral and morphological analysis.

Characterization

Ultraviolet (UV)-visible absorption spectra of the samples have been measured on a Shimadzu UV-visible V-530A spectrophotometer in the range of 200-1000 nm. Fourier transform infrared (FT-IR) spectroscopy of the samples was examined on a Jasso FT-IR/4100 spectrophotometer with 4/cm resolution in the range of 4000-400/cm. The scanning electron microscope (SEM) analysis of samples was carried out using JEOL Model JSM - 6390LV SEM and transmission electron microscopy (TEM) characterization was performed using 300 KV JEOL-3011 high resolution TEM.

Biological assay

The antibacterial activity of the samples was evaluated by disc diffusion method [36] against two Gram-positive bacteria (*S. aureus, B. subtilis*) and two Gram-negative bacteria (*E. coli, S. typhi*). In this method, approximately 2.0×10^6 colony-forming units (CFU/ml) of the bacterial cultures were prepared by diluting with fresh Muller-Hinton broth and inoculated with nanoparticles and antibiotic on Muller-Hinton agar plates. Then, the concentration of samples is 40 mg/disc was loaded on 6 mm sterile disc and placed on the surface of the cultured agar plates to get diffusion. The plates were kept for incubation at 37°C for 24 hrs. Bactericidal activity with respect to zone of inhibition was also calculated using an antibiotic zone scale (HiMedia). Chloramphenicol was used as standard antibiotics for the pathogenic microorganism.

The antifungal activity was carried out by agar well diffusion method [37] against four funguses (*C. albicans*, *C. lunata*, *A. niger*, and *T. simii*). In this method, approximately 10^5 CFU/ml of inoculum suspension were prepared using Sabouraud's dextrose agar by suspending the fungal strains for 6 hrs. A total of 8 mm diameter wells were punched into the agar. The samples and solvent blanks (hydro alcohol and hexane) were filled in the wells of the agar and the fungal plates were incubated overnight at 37°C. After incubation, the zones of inhibition were measured and recorded. Standard antibiotic, fluconazole (concentration 1 mg/ml) was used as positive control.

RESULTS AND DISCUSSION

In general, in the preparation of nanoparticles, the color changes observed during the reaction is the important indications of the formation of nanoparticles. The reduction of manganese metal was confirmed by the color change from pale green to pale yellow and the stabilization of manganese nanoparticles are confirmed by the color change from yellowish to permanent reddish brown color.

UV-visible studies

UV-visible spectroscopy is most widely used technique to investigate the optical properties of the particles. Fig. 1 shows the UV-visible spectrum of synthesized MONPs. The spectra showed two important peaks situated at about 360 nm and 215 nm. The first peak (360 nm) was corresponding to the absorption maxima of manganese nanoparticles [38] and the second peak (215 nm) was probably observed by the aggregation of formed nanoparticles, which could be occurred due to the oxidation of nanoparticles and lying in the lower region. Fig. 2 shows the UV-visible spectrum of curcumininaniline functionalized MONPs. This spectrum showed three important peaks at 401 nm, 300 nm, and 225 nm. Here, the weak broad band exhibited at 401 nm which could be assigned to the interaction of curcumininaniline with MONPs. The sharp peak observed at 300 nm on the spectra of MNCA which belongs to the absorption of manganese nanoparticles and the other peak exhibited at 225 nm may be due to the formation of nanoparticles aggregation.

FT-IR studies

FTIR spectroscopy was carried out to establish the purity and nature of MONPs as synthesized by green synthesis method. Fig. 3 shows the FT-IR spectrum of synthesized MONPs. From the data obtained, the peaks observed in the wave regions around 3735-3650/cm could be assigned to the –OH (free) stretching of water or ethanol present in the system. The weak broad band in the range of 2935/cm which is assigned to C-H stretching of curcumin moiety. The C=O stretching was observed at 1704/cm and the three characteristic peaks in the range of 1574-1515/cm confirms the aromatic unsaturation (C=C) of the stabilized curcumin system and observed as multiple bands. The absorption peak at 1393/cm symbolized the C-H bending of adsorbed water of MONPs. The (C-O) stretching bands belongs to curcumin was assigned by the peaks found at 1026/cm and 1160/cm.

In the case of curcumininaniline functionalized MONPs (Fig. 4), the peak observed at 3675/cm which can be assigned to the O-H (free) stretching of water or ethanol present in the system. The very broad peak observed in the region of 3372/cm due to the stretching of O-H group bonded with the aromatic system of curcumininaniline. The major absorption bands observed by MNCA are followed, C-H stretching of curcumin system at 2922/cm, C=O vibration band at 1704/cm. The presence of aromatic C=C stretching, aromatic C-H bending, C-O bands stretching, and alkene C-H bending belongs to the curcumininaniline system are confirmed by the peaks raised at 1575/cm/1514/cm, 1385/cm, and 1200-1000/cm, respectively. The new peak exhibited at 2545/cm which could be due to the biofunctionalization of MONPs which was bonded with oxygen atom.

Oxides and hydroxides of metal nanoparticles generally give absorption peak in the fingerprint region, i.e., below wavelength of 1000/cm arising due to interatomic vibrations [39-41]. According to the results reported in literature, synthesized MONPs exhibited the two significant absorption peaks at 901/cm and 730/cm (Fig. 3) are corresponds to characteristic stretching bands of O-Mn-O and biofunctionalized manganese nanoparticles were observed the O-Mn-O stretching bands at 830/cm and 805/cm (Fig. 4) which demonstrated the presence of the Mn-O metal stretching in the both samples as well as the presence of curcumininaniline system in biofunctionalized MONPs.

SEM studies

Synthesized MONPs and curcumininaniline functionalized nanoparticles were analyzed for the structure and morphology studies using SEM at different magnification levels. The SEM image of MONPs is shown in Fig. 5a. It can be viewed that the MONP formed is in the form of nearly nanosphere morphology, which exist in contact with each other. SEM image of biofunctionalized MONPs is shown in Fig. 5b. It is found that the MNCA was mostly appeared aggregated as sphere shapes. The slight agglomeration is due to the nanoparticles oxidation.

TEM studies

TEM is used to obtain a clear size, shape, and structural image of the nanoparticles. Fig. 6a shows the TEM image of MONPs. TEM images

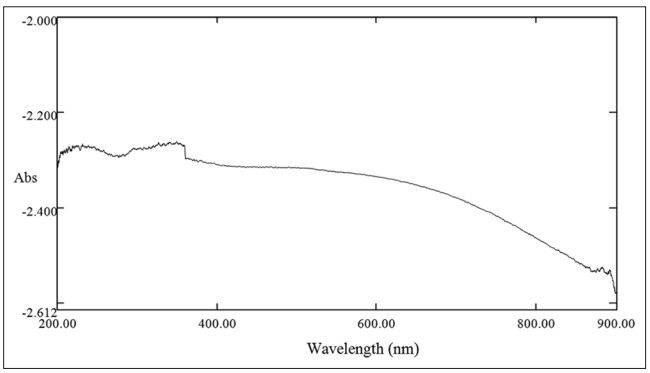

Fig. 1: Ultraviolet-visible spectra of manganese oxide nanoparticles

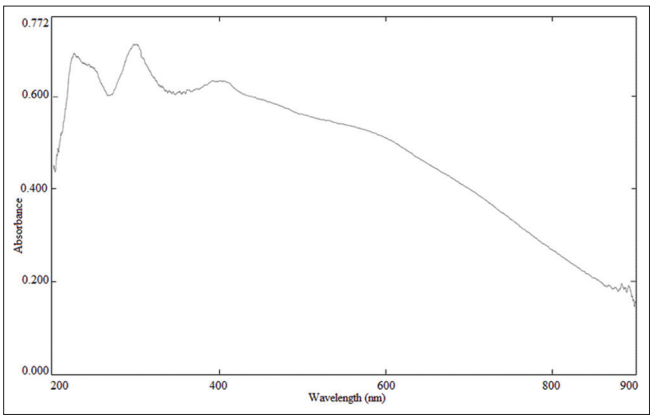

Fig. 2: Ultraviolet-visible spectra of biofunctionalized manganese oxide nanoparticles

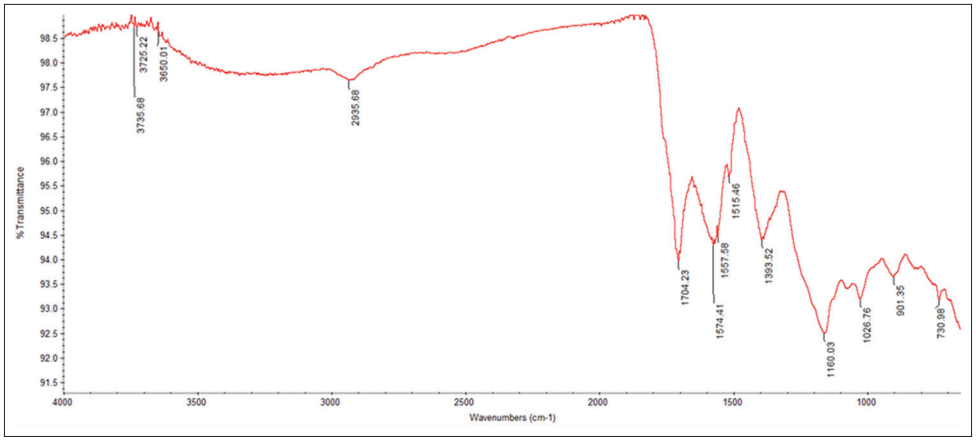

Fig. 3: Fourier transform infrared spectra of manganese oxide nanoparticles

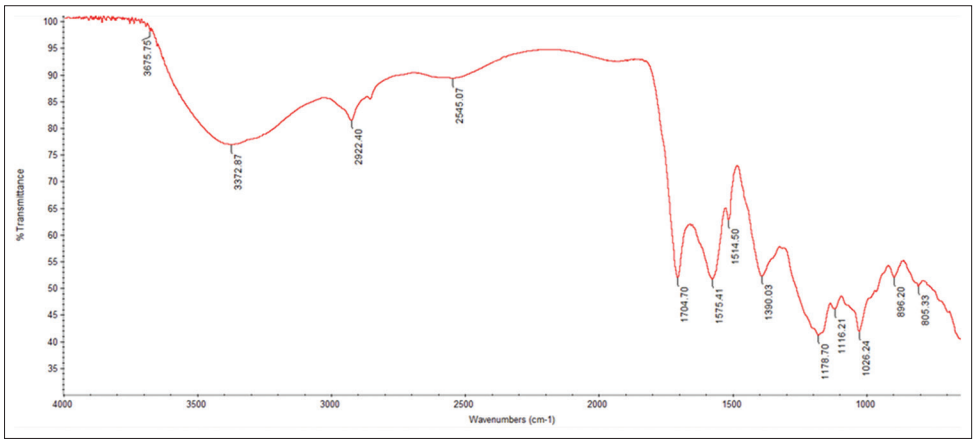

Fig. 4: Fourier transform infrared spectra of biofunctionalized manganese oxide nanoparticles scanning electron microscope studies

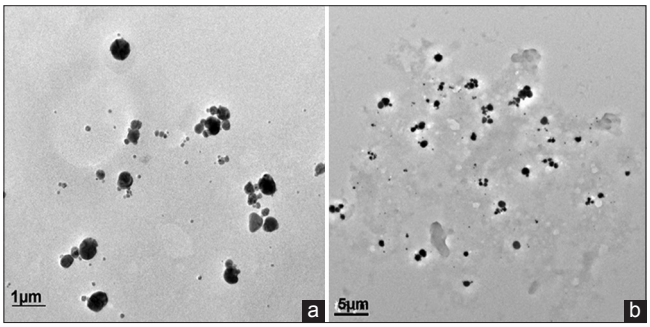

Fig. 5: Scanning electron microscope image of (a) manganese oxide nanoparticles; (b) biofunctionalized manganese oxide nanoparticles

of MONP reveals that the size of the nanoparticles to be <50±5 nm with clear eclipsed and spherical morphology. Fig. 6b shows the TEM image of curcumininaniline functionalized MONPs. TEM images of MNCA show that the particles formed are of spherical morphology and clearly dispersed. The average crystallite size of particles in the range of 50±10 nm. Based on our morphological studies, it is revealed that means particle size is increased after functionalization process which means the particles are tending to agglomeration and observed the increase in the size of particles.

Antimicrobial activity

The antibacterial activities of nonfunctionalized and curcumininaniline functionalized MONPs against two Gram-positive (*S. aureus* and *B. subtilis*) and two Gram-negative bacteria (*E. coli* and *S. typhi*) were evaluated. The result of antibacterial activity of samples is compared to a commercial antibiotic chloramphenicol and their efficiency is discussed (Table 1).

From Table 1 results, the antibacterial activity results revealed that zone of inhibition produced by the biofunctionalized MONPs against bacterial strains was extremely higher when compared to nonfunctionalized MONPs. The nonfunctionalized MONPs were observed lower inhibition activity against both Gram-negative bacterial species, i.e., *E. coli* and *S. typhi* as well as Gram-positive *B. subtilis*. However, it has shown somehow reasonable activity against *E. coli.* MONP has found that moderate activity against *S. aureus* only. Particularly, its zone of inhibition value is higher than standard drug. In the case of curcumininaniline functionalized MONPs, there is a noticeable inhibition zone results were displayed against all bacterial species. It is found that MNCA has shown superior antibacterial activity than nonfunctionalized nanoparticles against both Gram-positive and Gram-negative bacteria. Especially, it showed an excellent activity against *S. aureus, B. subtilis*, and *S. typhi* strains which considerably higher than MONP as well as standard drug. Interestingly, it has shown reasonable activity nearly similar to standard drug against *E. coli*. Therefore, it can be concluded that curcumininaniline functionalized MONPs were showing significant performance against all species than the nonfunctionalized form and also standard drug.

The synthesized nonfunctionalized manganese oxide and biofunctionalized MONPs were determined for their antifungal activity against four fungal strains *C. albicans*, *C. lunata*, *A. niger*, and *T. simii*. The antifungal zone results were compared with standard antifungal drug fluconazole (Table 2).

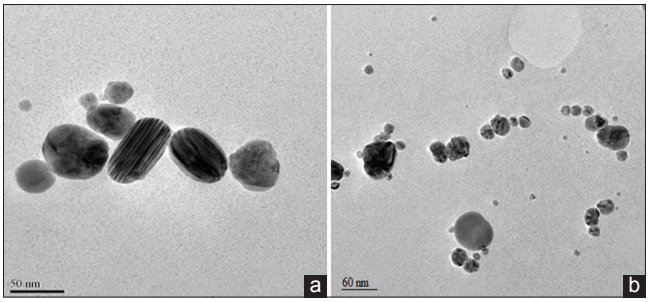

Fig. 6: Transmission electron microscopy image of (a) manganese oxide nanoparticles; (b) biofunctionalized manganese oxide nanoparticles

Table 1: Evaluation of antibacterial effectiveness using zone of inhibition test method

Bacterial species	Zone of inhibition diameter (mm/sample)		
	C	MONP	MNCA
S. aureus	13	15	18
B. subtilis	15	08	19
E. coli	11	09	10
S. typhi	14	10	19

S. aureus: Staphylococcus aureus, B. subtilis: Bacillus subtilis, E. coli: Escherichia coli, S. typhi: Salmonella typhi, C: Standard drug, MONP: Manganese oxide nanoparticles, MNCA: Biofunctionalized manganese oxide nanoparticles

Table 2: Evaluation of antifungal effectiveness using zone of inhibition test method

Fungal species	Zone of inhibition diameter (mm/sample)		
	C	MONP	MNCA
C. albicans	16	16	19
C. lunata	15	17	15
A. niger	15	13	13
T. simii	13	14	16

C. albicans: *Candida albicans*, *C. lunata*: *Curvularia lunata*, *A. niger*: *Aspergillus niger*, *T. simii: Trichophyton simii*, C: Standard drug, MONP: Manganese oxide nanoparticles, MNCA: Biofunctionalized manganese oxide nanoparticles

From Table 2, antifungal activity of both MONP and MNCA have showed significant inhibition zone results against all pathogens tested here. There was an appreciable result found for nonfunctionalized MONPs, which shows the inhibition activity relatively increased against *C. albicans, C. lunata*, and *T. simii* pathogens. However, curcumininaniline functionalized MONPs were acted as high resistance to *C. albicans*, *C. lunata*, and *T. simii* fungal species which were higher than MONP. Surprisingly, the resistance activity of MNCA was certainly higher than the control against above-mentioned pathogens. Both nanoformulations are shown moderate inhibition activity against *T. simii*. MONP showing slightly higher activity than MNCA against *C. lunata* but the overall inhibition activity of MNCA was considerably higher than nonfunctionalized form as well as standard drug.

From the zone of inhibition studies there is an evidence that curcumininaniline play a key role in the enhancement of the antibacterial and antifungal activity of biofunctionalized MONPs. The enhancement in the antimicrobial activity is due to the fact that the presence of modified curcumin biomaterial, which possess high resistance to microbes. In addition, the existence of azomethine group in curcumininaniline produced microbial resistance enormously would evidently result in greater changes of activity. Manganese nanoparticles hold large surface-to-volume ratio that is helpful in the effective functionalization of curcumin biomaterial. Moreover, the high surface-to-volume ratio of manganese nanoparticles induced the interaction with the surface of microbial strains and biologically activated material existing on the nanomaterials acted as highly resistive to pathogens and resulting remarkable antimicrobial activity. As a result of this, we found that the functionalized curcumininaniline presence in the MNCA acted as a key role in the increment of inhibition activity against pathogens than the nonfunctionalized MONP.

CONCLUSION

This investigation was performed to find out an effective microbial active agent in the different approach by synthesizing MONPs, which was functionalized with bioactive curcumininaniline biomaterial to enhance the activity which was prepared by the modification of curcumin. MONPs were prepared using lemon extract and curcumin extract as a reducer and stabilizer, respectively. This bio-green synthesis process was appropriately simple, low cost, nontoxic, and eco-friendly. The spectral studies UV-visible and FT-IR are confirmed the formation and functionalization of nanoparticles. Morphological studies are exposed that the formed MONPs are of eclipsed spherical morphology with size about 50±5 nm and biofunctionalized nanoparticles are of agglomerated spherical morphology with size around 50±10 nm. The zone of inhibition activity results was represented that biofunctionalized form has shown superior activity than nonfunctionalized MONPs and also standard drugs against *S. aureus, B. subtilis, S. typhi* bacterial strains and *C. albicans, C. lunata*, *T. simii* fungal species. As a result of this, we can conclude that curcumininaniline functionalized MONPs are better in the bactericidal activity by resisting bacterial growth when compared with nonfunctionalized nanoparticles. Our findings may lead to valuable inventions in the field of antimicrobial systems as well as medical devices in the future.

ACKNOWLEDGMENTS

We thank AMET University, Chennai, India for their support to do this work. We gratefully acknowledge SAIF, North-Eastern Hill University (NEHU), Shillong for TEM analysis and Nanotechnology Research Centre, SRM University, Chennai for SEM analysis facilities. We thank PG and Research Department of Chemistry, V.O. Chidambaram College, Tuticorin for providing IR spectral analysis facility and Department of Chemistry, SFR College for women, Sivakasi for providing UV analysis facility.

REFERENCES

1. Lakshmi VJ, Kannan KP. Biosynthesis of gold nanoparticles by biosorption using neosartorya udagawae: Characterization and *in vitro* evaluation. Int J Pharm Sci 2016;8(11):108-13.
2. White RJ, Luque R, Budarin VL, Clark JH, Macquarrie DJ. Supported metal nanoparticles on porous materials. Methods and applications. Chem Soc Rev 2009;38(2):481-94.
3. Rao CN, Vivekchand SR, Biswas K, Govindaraj A. Synthesis of inorganic nanomaterials. Dalton Trans 2007;(34):3728-49.
4. Logeswari P, Silambarasan S, Jayanthi A. Synthesis of silver nanoparticles using plants extract and analysis of their antimicrobial property. J Saudi Chem Soc 2015;19(3):311-7.
5. Anastas PT, Warner JC. Green Chemistry: Theory and Practice. 1st ed. New York: Oxford University Press Publishers; 1998.
6. Mudshinge SR, Deore AB, Patil S, Bhalgat CM. Nanoparticles: Emerging carriers for drug delivery. Saudi Pharm J 2011;19(3):129-41.
7. De Jong WH, Borm PJ. Drug delivery and nanoparticles: Applications and hazards. Int J Nanomedicine 2008;3(2):133-49.
8. Seabra AB, Duran N. Nanotoxicology of metal oxide nanoparticles. Metals 2015;5(2):934-75.
9. Mohammad JH, Katharina MF, Ashkarran AA, De Aberasturi DJ, De Larramendi IR, Rojo T, *et al*. Antibacterial properties of nanoparticles. Trends in Biotechnol 2012;30(10):499-511.
10. Mukherjee A, Sadiq IM, Prathna TC, Chandrasekaran N, editors. Antimicrobial activity of aluminium oxide nanoparticles for potential clinical Applications. Spain: Formatex Research Center; 2011. p. 245-51.
11. Jones N, Ray B, Ranjit KT, Manna AC. Antibacterial activity of ZnO nanoparticle suspensions on a broad spectrum of microorganisms. FEMS Microbiol Lett 2008;279(1):71-6.]

12. Frey NA, Peng S, Cheng K, Sun S Magnetic nanoparticles: Synthesis, functionalization, and applications in bioimaging and magnetic energy storage. Chem Soc Rev 2009;38(9):2532-42.
13. Predoi D, Ciobanu CS, Radu M, Costache M, Dinischiotu A, Popescu C, *et al*. Hybrid dextran-iron oxide thin films deposited by laser techniques for biomedical applications. Mater Sci Eng C 2012;32(2):296-302.
14. Mona MA, Amira MM. Solid lipid nanoparticles and nanostructured lipid carriers of tolnaftate: Design, optimization and *in vitro* evaluation. Int J Pharm Sci 2016;8:380-5.
15. Estelrich J, Sánchez-Martín MJ, Busquets MA. Nanoparticles in magnetic resonance imaging: From simple to dual contrast agents. Int J Nanomedicine 2015;10:1727-41.
16. Wei W, Cui X, Chen W, Ivey DG. Manganese oxide-based materials as electrochemical supercapacitor electrodes. Chem Soc Rev 2011;40(3):1697-721.
17. Song MK, Zhang Y, Cairns EJ. A long-life, high-rate lithium/sulfur cell: A multifaceted approach to enhancing cell performance. Nano Lett 2013;13(12):5891-9.
18. Deng QF, Ren TZ. Mesoporous manganese oxide nanoparticles for the catalytic total oxidation of toluene. React Kinet Mech Catal 2013;108(2):507-18.
19. Miyamoto Y, Kuroda Y, Uematsu T, Oshikawa H, Shibata N, Ikuhara Y, *et al.* Synthesis of ultrasmall Li-Mn spinel oxides exhibiting unusual ion exchange, electrochemical, and catalytic properties. Sci Rep 2015;5:15011.
20. Pradeep Kumar BM, Sriram K, Harikrishna R, Udayasankara TH, Shivaprasad KH, Nagabhushana BM. Synthesis characterization of nano MnO_2 and its adsorption characteristics over an Azo dye. Res Rev J Mater Sci 2014;2(1):27-31.
21. El-Deab MS, Ohsaka T. Manganese oxide nanoparticles electrodeposited on platinum are superior to platinum for oxygen reduction. Angew Chem Int Ed Engl 2006;45(36):5963-6.
22. Li WN, Yuan JK, Gomez-Mower S, Xu LP, Sithambaram S, Aindow M, *et al*. Hydrothermal synthesis of structure- and shape-controlled manganese oxide octahedral molcular sieve nanomaterials. Adv Funct Mater 2006;16(9):1247-53.
23. Kumar SS. Biological and Pharmaceutical Nanomaterials. 1st ed. Weinheim: Wiley-VCH Verlag GmbH Co., KGaA; 2005.
24. Goesmann H, Feldmann C. Nanoparticulate functional materials. Angew Chem Int Ed 2010;49(8):1362-95.
25. Veiseh O, Gunn JW, Zhang M. Design and fabrication of magnetic nanoparticles for targeted drug delivery and imaging. Adv Drug Deliv Rev 2010;62(3):284-304.
26. Mishra RP, Javed I. *In vitro* activity of medicinal plants against some bacterial and fungal isolates. Asian J Pharm Clin Res 2015;8(1):225-30.
27. Katsori AM, Chatzopoulou M, Dimas K, Kontogiorgis C, Patsilinakos A, Trangas T, *et al.* Curcumin analogues as possible anti-proliferative & anti-inflammatory agents. Eur J Med Chem 2011;46(7):2722-35.
28. Tharakan ST, Inamoto T, Sung B, Aggarwal BB, Kamat AM. Curcumin potentiates the antitumor effects of gemcitabine in an orthotopic model of human bladder cancer through suppression of proliferative and angiogenic biomarkers. Biochem Pharmacol 2010;79:218-28.
29. Gangwar RK, Dhumale VA, Kumari D, Nakate UT, Gosavi SW, Sharma RB, *et al*. Conjugation of curcumin with PVP capped gold nanoparticles for improving bioavailability. Mater Sci Eng C 2012;32(8):2659-63.
30. Moussawi RN, Patra D. Modification of nanostructured ZnO surfaces with curcumin: Fluorescence-based sensing for arsenic and improving arsenic removal by ZnO. RSC Adva 2016;6(21):17256-68.
31. El Khoury E, Abiad M, Kassaify ZG, Patra D. Green synthesis of curcumin conjugated nanosilver for the applications in nucleic acid sensing and anti-bacterial activity. Colloids Surf B Biointerfaces 2015;127:274-80.
32. Garcia OB, Castillo J, Marin JR, Ortuno A, Del Rio JA. Uses and properties of citrus flavonoids. J Agric Food Chem 1997;45(12):4505-15.
33. Vinson JA, Su X, Zubik L, Bose P Phenol antioxidant quantity and quality in foods: Fruits. J Agric Food Chem 2001;49(11):5315-21.
34. Manjunath MN, Sattigeri VD, Nagaraj KV. Curcumin in turmeric. Spice India 1991;4(3):7-9.
35. Jayandran M, Haneefa MM, Balasubramanian V. Synthesis, characterization and biological activities of turmeric curcumin schiff base complex. Int J Chem Nat Sci 2014;2(5):157-63.
36. Bauer AW, Kirby WM, Sherris JC, Turck M Antibiotic susceptibility testing by a standardized single disk method. Am J Clin Pathol 1966;45(4):493-6.
37. Gomes BP, Ferraz CC, Vianna ME, Rosalen PL, Zaia AA, Teixeira FB, *et al. In vitro* antimicrobial activity of calcium hydroxide pastes and their vehicles against selected microorganisms. Braz Dent J 2002;13(3):155-61.
38. Sinha A, Singh VN, Mehta BR, Khare SK. Synthesis and characterization of monodispersed orthorhombic manganese oxide nanoparticles produced by *Bacillus* sp. cells simultaneous to its bioremediation. J Hazard Mater 2011;192(2):620-7.
39. Kang L, Zhang M, Liu ZH, Ooi K. IR spectra of manganese oxides with either layered or tunnel structures. Spectrochim Acta A Mol Biomol Spectrosc 2007;67(3-4):864-9.
40. Li L, Pan Y, Chen L, Li G. One-dimensional α-MnO_2: Trapping chemistry of tunnel structures, structural stability and magnetic transitions. Solid State Chem 2007;180(10):2896-904.
41. Potter RM, Rossman GR. The tetravalent manganese oxides: Identification, hydration, and structural relationships by infrared spectroscopy. Am Mineral 1979;64(1-2):1199-218.